Structure and Dynamic Process of Two-Dimensional Monodendron Assembly

Jian-Ru Gong,[†] Sheng-Bin Lei, Li-Jun Wan,* Guo-Jun Deng,[†]
Qing-Hua Fan, and Chun-Li Bai*

*Center for Molecular Science, Institute of Chemistry, Chinese Academy of Sciences,
Beijing 100080, People's Republic of China*

Received March 12, 2003. Revised Manuscript Received June 3, 2003

The formation and structure of self-assembled monolayers of three monodendrons, 5-(benzyloxy)-isophthalic acid derivatives, bearing different alkyl substitutents on highly oriented pyrolytic graphite have been studied by scanning tunneling microscopy (STM). It is found that the arrangements of the molecules with one and two alkyl substituents are different, although the two molecules both form long-range ordered structures. For the derivative with three alkyl substituents, no ordered arrangement in a large area was observed. The interaction mechanism of the self-assembly monolayer is discussed. As an example, the formation and dynamic process of the adlayer of monodendron derivative with one alkyl chain was directly investigated by STM. In the same scanning area, time-dependent disorder−order transition was observed. The result can be explained by the minimization of the free energy in the whole system.

Introduction

The control of surface chemistry has become increasingly important in the preparation of materials and devices at the nanometer scale. Self-assembled monolayers (SAMs), generated by the adsorption of organic molecules onto solid substrates, have potential applications from nanotechnology to fundamental surface science because of their stable and densely packed structures, their controllable surface functional groups and chemical properties, and their simple and rapid preparation.[1]

Dendrimers, named for the treelike branched structure of the polymer chains that radiate from the molecule's central core, represent a key stage in the ongoing evolution of macromolecular chemistry. The highly compact and globular shape, as well as the uniform size and plurifunctionality of dendrimers, makes them ideal molecular building blocks for the construction of complex molecular, macromolecular, and supramolecular functional nanotechnological applications. By manipulating the molecular structures generation by generation, chemists can tailor the properties of the overall dendrimers.[2] One of the best examples of tailoring so far is the creation of an electric-potential gradient between a dendrimer's inner and outer generations. The irradiation of multiple donating chromophores around a single acceptor amplifies the emission of the focal acceptor due to the highly efficient energy transfer that occurs within such a molecule, and this is a useful

step toward the goal of efficient light-harvesting and artificial photosynthesis.[3] Dendritic macromolecules have been blended into organic light-emitting diodes (OLEDs) as either a hole-transporting component or electron-transporting component or even as single-component emitters.[4,5] The dendritic core also offers a unique microenvironment, making them interesting candidates for host−guest chemistry.[6] They can be used as sensors, catalysts, gene delivery agents, and drug carriers for controlled release and site-specific delivery. Monolayers of dendrimers that can be used as resists for scanning probe lithography have been fabricated[7] and polyamidoamine dendrimers (PAMAM) have been used as inks for contact printing and "dip-pen nanolithography". These techniques may find potential application in the construction of nanodevices.[8,9] Templates for the preparation of nanoparticles such as Cu, Pd, and Pt[10] can also be made by dendrimers.

Combining molecular self-assembly technique with dendrimer chemistry, some research groups have addressed the thin films on surfaces,[11] with several studies focusing on the preparation of multilayer films,[12−14] by

* To whom correspondence should be addressed. E-mail: wanlijun@iccas.ac.cn (L.-J. Wan); clbai@iccas.ac.cn (C.-L. Bai).Tel./Fax: +86-10 6255 8934.
† Also in Graduate School of Chinese Academy of Sciences, Beijing, China.

(1) Zhang, H.; Grim, P. C. M.; Liu, D. J.; Vosch, T.; DeFeyter, S.; Wiesler, U.-M.; Berresheim, A. J.; Müllen, K.; Van Haesendonck, C.; Vandamme, N.; De Schryver, F. C. *Langmuir* **2002,** *18,* 1801.
(2) Christopher, G. *Nature* **2002,** *415,* 487.
(3) Adronov, A.; Gilat, S. L.; Fréchet, J. M. J.; Ohta, K.; Neuwahl, F. V. R.; Fleming, G. R. *J. Am. Chem. Soc.* **2000,** *122,* 1175.
(4) Wang, P. W.; Liu, Y. J.; Devadoss, C.; Bharathi, P.; Moore, J. S. *Adv. Mater.* **1996,** *8,* 237.
(5) Halim, M.; Pillow, J. N. G.; Samuel, I. D. W.; Burn, P. L. *Adv. Mater.* **1999,** *11,* 371.
(6) Bosman, A. W.; Janssen, H. M.; Meijer, E. W. *Chem. Rev.* **1999,** *99,* 1665.
(7) Tully, D. C.; Wilder, K.; Fréchet, J. M. J.; Trimble, A. R.; Quate, C. F. *Adv. Mater.* **1999,** *11* (4), 314.
(8) Li, H. W.; Kang, D. J.; Blamire, M. G.; Huck, W. T. S. *Nano Lett.* **2002,** *2* (4), 347.
(9) McKendry, R.; Huck, W. T. S.; Weeks, B.; Fiorini, M.; Abell, C.; Rayment, T. *Nano Lett.* **2002,** *2* (7), 713.
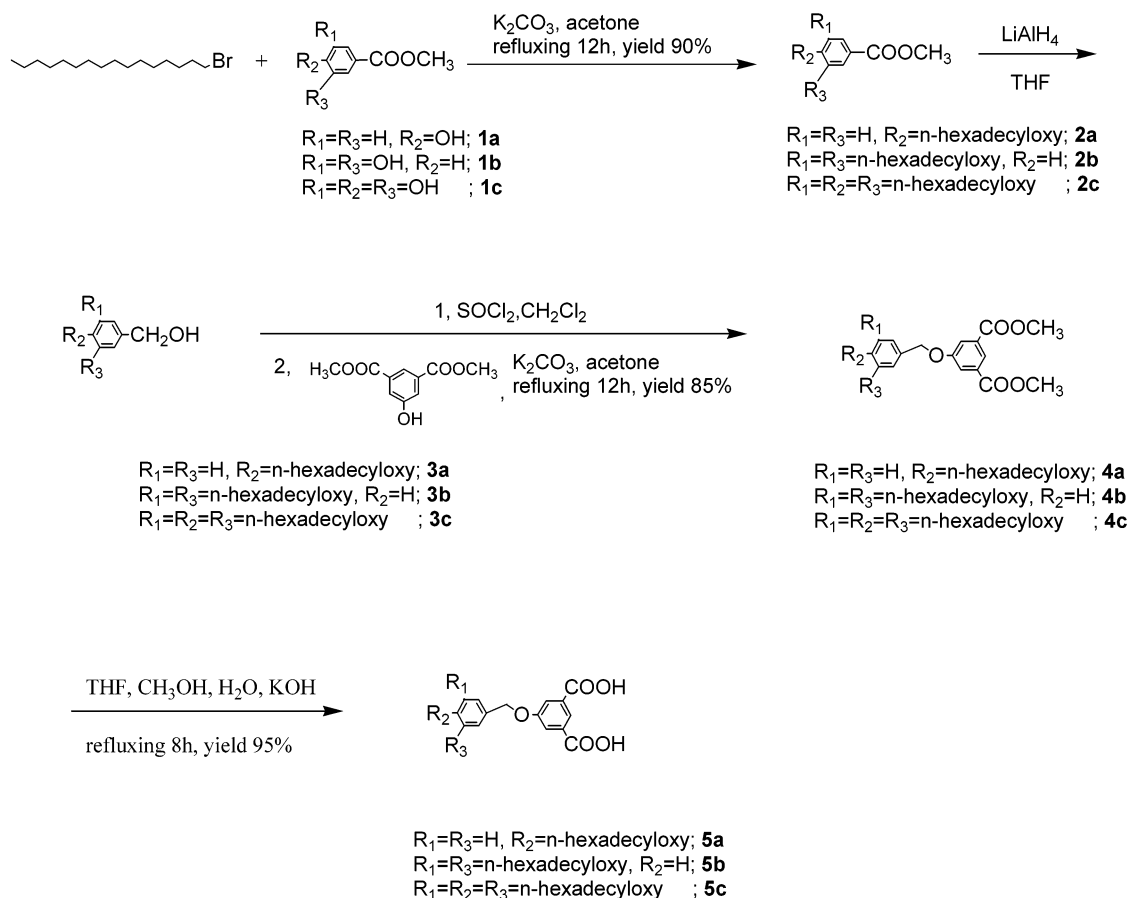(10) Zhao, M.; Crooks, R. M. *Angew. Chem., Int. Ed.* **1999,** *38,* 364.
(11) Grayson, S. M.; Fréchet, J. M. J. *Chem. Rev.* **2001,** *101,* 3819.
(12) Tsukruk, V. V. *Adv. Mater.* **1998,** *10,* 253.
(13) Watanabe, S.; Regen, S. L. *J. Am. Chem. Soc.* **1994,** *116,* 8855.
(14) Yoon, H. C.; Kim, H. S. *Anal. Chem.* **2000,** *72,* 922.

Scheme 1

$R_1=R_3=H$, $R_2=OH$: **1a**
$R_1=R_3=OH$, $R_2=H$: **1b**
$R_1=R_2=R_3=OH$; **1c**

K$_2$CO$_3$, acetone
refluxing 12h, yield 90%

$R_1=R_3=H$, $R_2=$n-hexadecyloxy; **2a**
$R_1=R_3=$n-hexadecyloxy, $R_2=H$; **2b**
$R_1=R_2=R_3=$n-hexadecyloxy ; **2c**

LiAlH$_4$

THF

$R_1=R_3=H$, $R_2=$n-hexadecyloxy; **3a**
$R_1=R_3=$n-hexadecyloxy, $R_2=H$; **3b**
$R_1=R_2=R_3=$n-hexadecyloxy ; **3c**

1, SOCl$_2$,CH$_2$Cl$_2$

2, H$_3$COOC COOCH$_3$ OH , K$_2$CO$_3$, acetone refluxing 12h, yield 85%

$R_1=R_3=H$, $R_2=$n-hexadecyloxy; **4a**
$R_1=R_3=$n-hexadecyloxy, $R_2=H$; **4b**
$R_1=R_2=R_3=$n-hexadecyloxy ; **4c**

THF, CH$_3$OH, H$_2$O, KOH

refluxing 8h, yield 95%

$R_1=R_3=H$, $R_2=$n-hexadecyloxy; **5a**
$R_1=R_3=$n-hexadecyloxy, $R_2=H$; **5b**
$R_1=R_2=R_3=$n-hexadecyloxy ; **5c**

using the analytic methods of transmission electron microscopy (TEM),[15] scanning electron microscopy (SEM),[16] X-ray diffraction (XRD),[17] and X-ray photoelectron spectroscopy (XPS).[18] Although many techniques are useful for probing the structure of SAMs, only scanning tunneling microscopy (STM) and related methods have the potential to provide high-resolution imaging and measurement of surface topography and properties on a molecular and even atomic scale due to the very localized nature of the probing. Perhaps even more important, the dynamics of the adsorption process and reaction can be studied in real space and time.[19] Using STM, the surface assembly of disklike units of the first generation of monodendron 3,4,5-tridecyloxybenzoic acid, the second generation of modified Fréchet-type acid monodendron,[20] and the different arrangements of monodendrons induced by the functional groups at the focal point were previously studied by our group.[21]

Until now, these studies have considered only the time-averaged static characteristics and neglected the dynamic characteristics of these adlayers. Apart from being of utmost interest in itself, the dynamic information gained from such STM "movies" is also very decisive for a full understanding of the resulting static surface structures.[22] Furthermore, by analyzing a large number of pictures (with atomic resolution) concerning dynamic processes on surfaces, it is possible to study fundamental physical and chemical issues such as diffusion constants and interaction energies by STM measurements.

Herein we present an STM study on the assembly of the first generation monodendrons, 5-(benzyloxy)-isophthalic acid derivatives, bearing a different number of long alkyl chains. In addition, an observation on the adsorption dynamic process of the assembly is provided.

Experimental Section

The compound **5a** (**5b**, **5c**) was synthesized as follows: etherification of 1-bromohexadecane with 4-hydroxybenzoate **1a** (**1b**, **1c**) followed by reduction with LiAlH$_4$ gave **3a** (**3b**, **3c**) in high reaction yield. **3a** (**3b**, **3c**), after being chlorated and etherificated, gave **4a** (**4b**, **4c**) in 85% yield and then **5a** (**5b**, **5c**) was synthesized in >95% yield by hydrolyzing **4a** (**4b**, **4c**) (Scheme 1).

The **5a** (**5b**, **5c**) monolayer physisorbed from toluene (HPLC grade, Aldrich) was obtained by depositing a drop (~2 μL) of solution containing the compound to be studied (<1 mM) on a freshly cleaved atomically flat surface of highly oriented pyrolytic graphite (HOPG) (quality ZYB, Digital Instruments).

The STM characterization was performed on a Nanoscope IIIa SPM (Digital Instruments, Santa Barbara, CA) in air after the droplet dried out. STM tips were mechanically cut Pt/Ir

(15) Hudson, S. D.; Jung, H.-T.; Percec, V.; Cho, W.-D.; Johansson, G.; Ungar, G.; Balagurusamy, V. S. K. *Science* **1997**, *278*, 449.
(16) Kakiuchi, T.; Sato, K.; Iida, M.; Hobara, D.; Imabayashi, S.-i.; Niki, K. *Langmuir* **2000**, *16*, 7238.
(17) Balagurusamy, V. S. K.; Ungar, G.; Percec, V.; Johansson, G. *J. Am. Chem. Soc.* **1997**, *119*, 1539.
(18) Folkers, J. P.; Laibinis, P. E.; Whitesides, G. M. *Langmuir* **1992**, *8*, 1330.
(19) McCarty, G. S.; Weiss, P. S. *Chem. Rev.* **1999**, *99*, 1665.
(20) Wu, P.; Fan, Q. H.; Deng, G. J.; Zeng, Q. D.; Wang, C.; Bai, C. L. *Langmuir* **2002**, *18*, 4342.
(21) Wu, P.; Fan, Q. H.; Zeng, Q. D.; Wang, C.; Deng, G. J.; Bai, C. L. *ChemPhysChem* **2002**, *7*, 633.

(22) Magnussen, O. M. *Chem. Rev.* **2002**, *102*, 679.

wire (90/10). All the STM images were recorded using the constant current mode. The specific tunneling conditions are given in the figure captions.

The STM images were recorded at both positive and negative sample bias, but no appreciable contrast variations were observed. Due to the higher quality, only the images taken at positive bias were presented. All STM images were acquired with the constant current mode and without further process such as filtering.

Results and Discussion

1. Self-assembly of 5a. Figure 1a shows the large uniform and well-ordered assembly of **5a**. It is noticed that the remarkably bright bands and dark stripes are alternating over the whole viewed area. A zoomed-in image (Figure 1b) reveals a closely packed arrangement of **5a** molecules on the graphite surface with submolecular resolution. Owing to the large electronic density of aromatic cores, the contrast of this part is higher than the alkyl chains in the image. The bright spots appearing with a measured size of 0.5 ± 0.1 nm in the image are assigned to the phenyl rings. Besides the bright dots, the darker regions in the image correspond to the alkyl groups of the molecules. The length of one alkyl chain and spacing of consecutive chains are measured to be 2.0 ± 0.1 and 0.5 ± 0.1 nm, respectively, which is consistent with the length of a hexadecane chain in its all trans planar zigzag conformation. The above measuring results reflect a molecular flat-lying geometry of **5a** with its phenyl ring and alkyl chain adsorbed parallel to the substrate. In the image, all the molecules are packed head (carboxyl)-to-head. For the existence of carboxyl groups, hydrogen bonds can be formed among molecules. An illustrative model for the molecular arrangement could be proposed based on the STM observation (Figure 1c). The 2D unit cell as marked on the molecular model composes two molecules with parameters $a = 4.5 \pm 0.1$ nm, $b = 1.2 \pm 0.1$ nm, and $\alpha = 87 \pm 2°$, which are in good agreement with the observed STM image. The image shows that the alkyl chains of the molecules are interdigitated over the full length in the lamellae. By interdigitattion of the alkyl chains, a close-packed arrangement of **5a** is realized. These space-filling properties of alkyl chains and planar aromatic cores minimize the free space per unit area within the monolayer on the graphite surface. This results in a maximum of the intermolecular and molecule/graphite interactions. In this way, a stable monolayer with a sufficiently low molecular lateral mobility is assembled, which is a prerequisite for high-quality STM imaging.[23] The formation of hydrogen bonding between the carboxyl groups also contributes to the stability of the assembly.

2. Self-assembly of 5b. A large-scale image of a well-ordered **5b** arrangement is exhibited in Figure 2a. Bearing no resemblance to **5a**, all the alkyl chains are packed tail-to-tail instead of interdigitation. Figure 2b shows a high-resolution image of **5b**. Along the lamella, some bright dots are orderly arranged. Adjacent to the bright dots, parallel alkyl chains are observed and the length of these alkane chains is in good agreement with the length of a hexadecyl chain in its all trans confor-
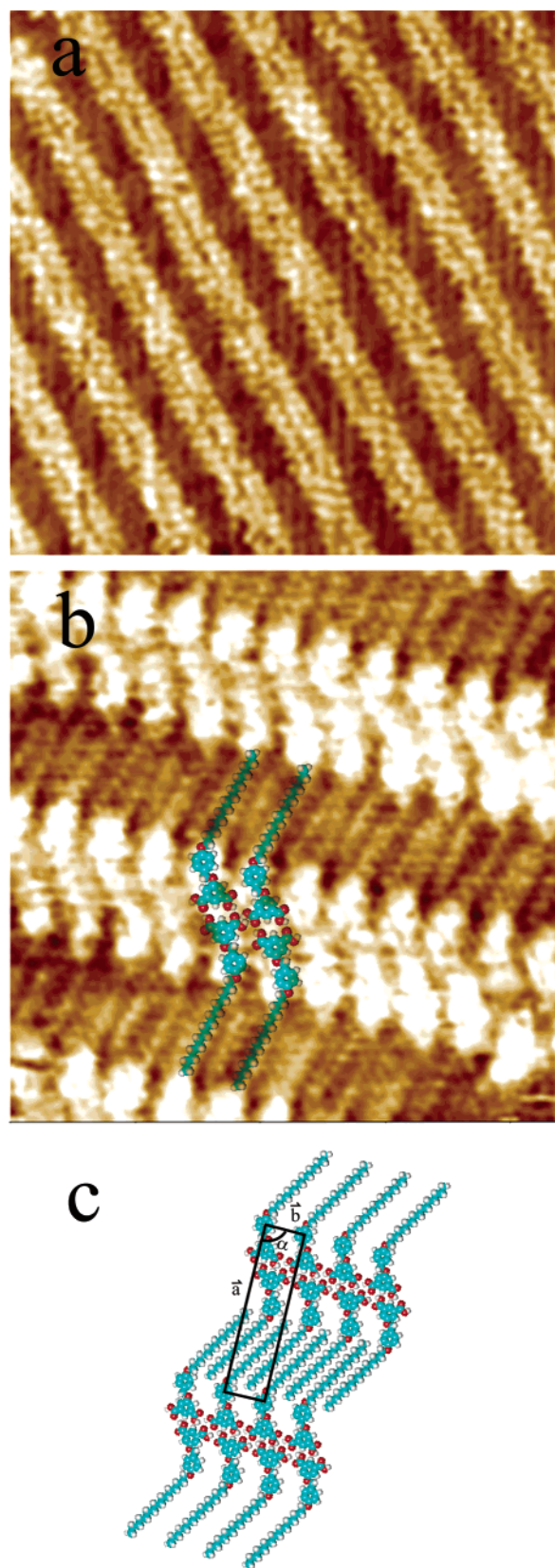
(23) Vanoppen, P.; Grim, P. C. M.; Rücker, M.; DeFeyter, S.; Moessner, G.; Valiyaveettil, S.; Müllen, K.; DeSchryver, F. C. *J. Phys. Chem.* **1996**, *100*, 19636.
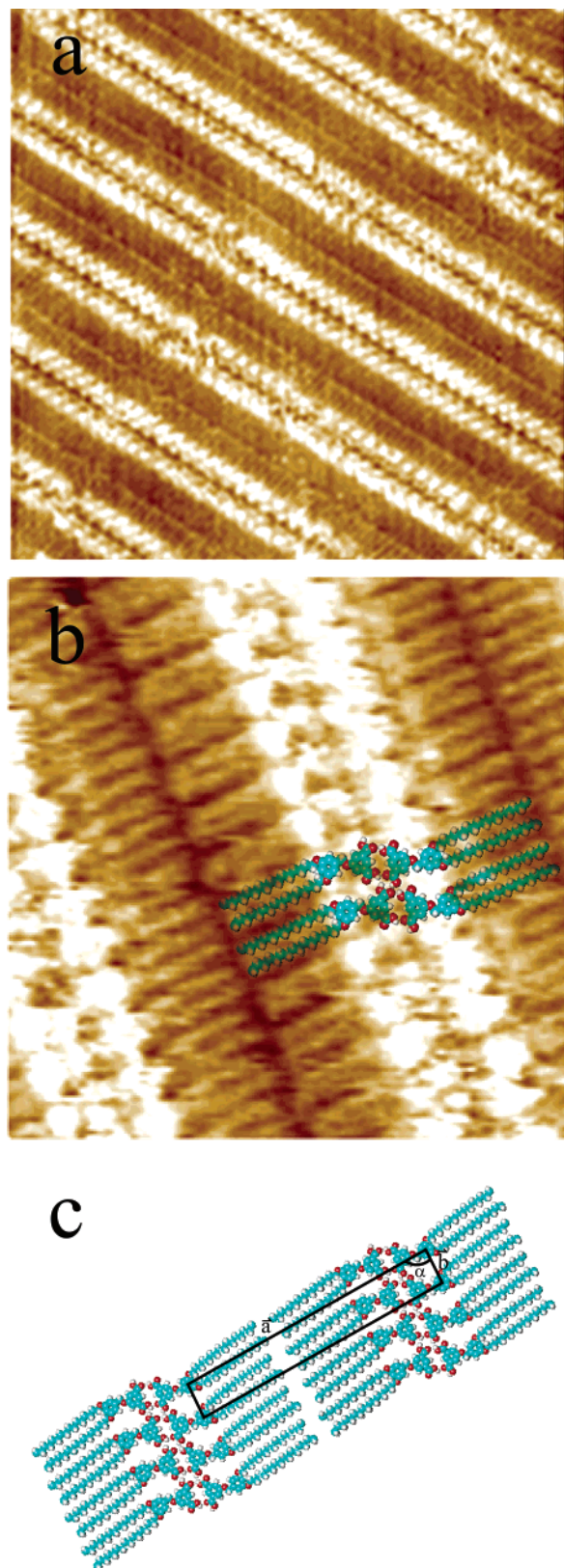

Figure 1. (a) STM image of a 50×50 nm^2 region of the assembly of **5a** in larger scale recorded with $V = 954$ mV and $I = 672$ pA. (b) STM image of a 11×11 nm^2 region of the assembly of **5a** in high resolution recorded with $V = 569$ mV and $I = 163$ pA. (c) Molecular model for the 2D packing of **5a** molecules and proposed unit cell. The unit cell contains two **5a** molecules with parameters $a = 4.5 \pm 0.1$ nm, $b = 1.2 \pm 0.1$ nm, and $\alpha = 87 \pm 2°$.
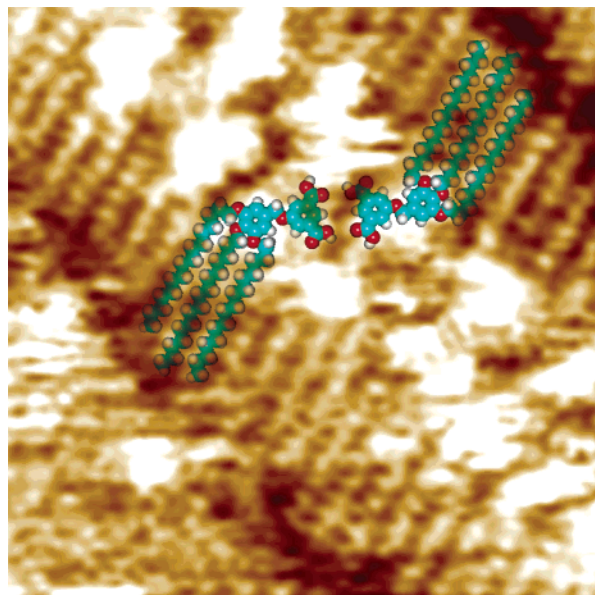
Figure 3. STM image of a 7×7 nm^2 region of the assembly of **5c** in high resolution recorded with $V = 479$ mV and $I = 254$ pA.

mation. In the image, all the molecules are densely packed head (carboxyl)-to-head. Two molecules compose one repeat unit. Dimensions of the unit cell are measured to be $a = 6.8 \pm 0.1$ nm, $b = 1.0 \pm 0.1$ nm, and $\alpha = 90 \pm 2°$ (Figure 2c). The intermolecular hydrogen bonds have a great stabilizing influence on the formation of 2D adlayers.

3. Self-assembly of 5c. STM investigation on the assembly of **5c** shows that the comblike assembling structure of **5c** adopts a packing motif similar to that of **5b**, but more disordered in the large-scale image. High-resolution image (Figure 3) reveals that some bright dots are loosely arrayed in the bright lamella. It is noticed that the alkyl chains are tilted with respect to the long axis of aromatic cores and the 127° angle is consistent with the optimized conformation of **5c**. The 2.0-nm length of the alkyl chain measured from the image is also in agreement with the length of a hexadecyl chain in its all trans conformation. The distance between two molecules along the stripes was measured to be 1.5 nm. Within this distance only three parallel alkyl tails can be arranged tightly on the surface with an average distance between the chains of at least 0.45 nm. The molecules are arranged head (carboxyl) to head. Through hydrogen bonding dimers are formed, illustrated by the overlaid molecular model, which is a basic building element for the adlayer.

4. Dynamic Process. STM images of organic molecules are usually interpreted as time averages over their molecular dynamics. Due to several important factors, there are substantial differences among the reported time scales for the adsorption process, ranging from seconds to 10$-$20 h.[24] In the following section, we will demonstrate a (slow) dynamic process.

Upon imaging the same region of a monolayer for a period of time, the image sequence shown in Figure 4 visualizes the dynamic process of **5a** from disordering to ordering. The large bright spot on the right of these

Figure 2. (a) STM image of a 42×42 nm^2 region of the assembly of **5b** in larger scale recorded with $V = 563$ mV and $I = 394$ pA. (b) STM image of a 11×11 nm^2 region of the assembly of **5b** in high resolution recorded with $V = 552$ mV and $I = 1.30$ nA. (c) Molecular model for the 2D packing of **5b** molecules and proposed unit cell. The unit cell contains two **5b** molecules with parameters $a = 6.8 \pm 0.1$ nm, $b = 1.0 \pm 0.1$ nm, and $\alpha = 90 \pm 2°$.
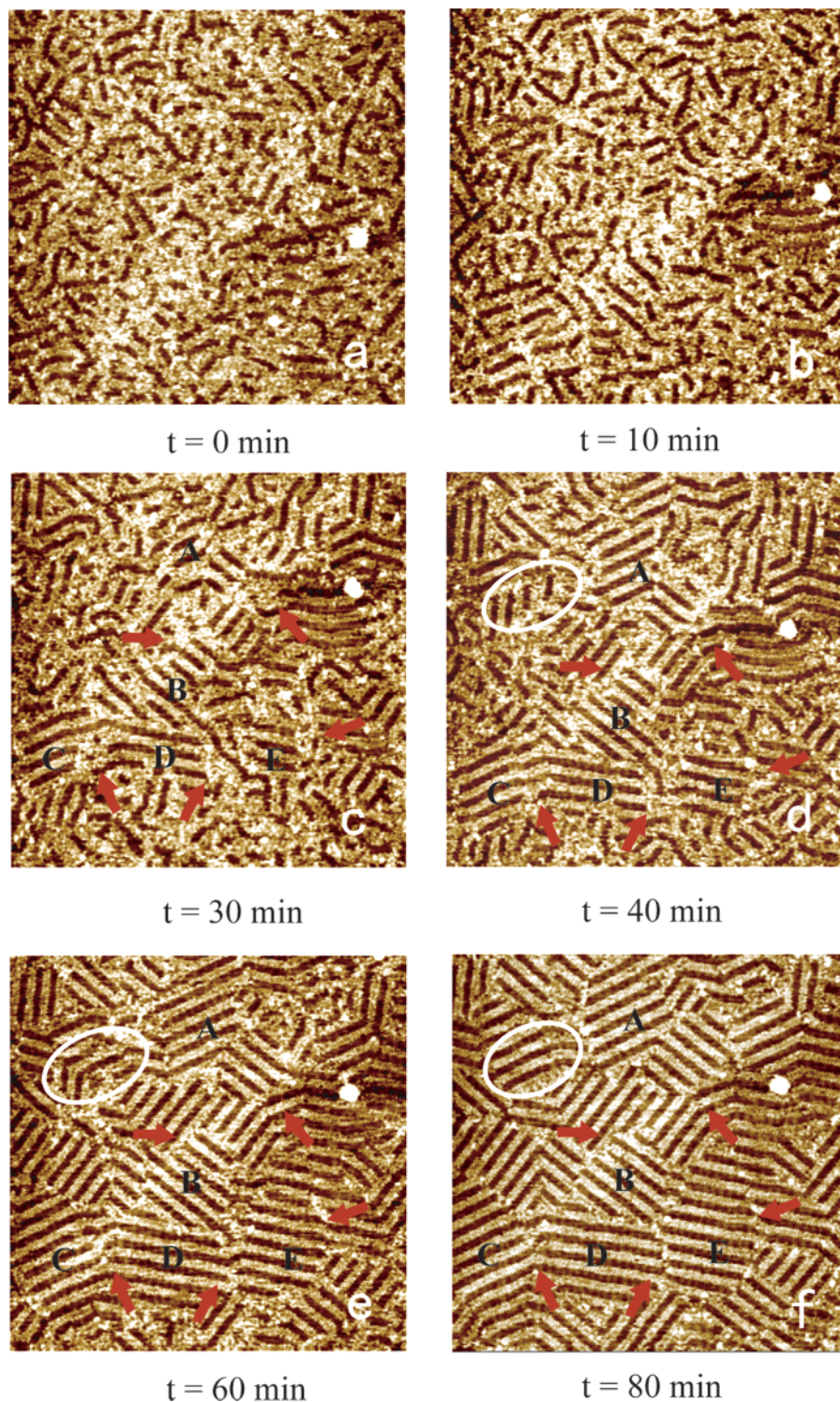
(24) Hu, K.; Bard, A. J. *Langmuir* **1998**, *14*, 4790.

Figure 4. Series of STM images of a 123 × 123 nm² region illustrating the dynamic process of **5a** from disordered to ordered assembly recorded with $V = 675$ mV and $I = 789$ pA. The time of the first image is arbitrarily set to zero. The encircled area indicates the reoriention of the molecules. The red arrows indicate the domain boundary where the molecules are highly movable during the ordering process.

images is used as a reference point to keep track of the progress of the dynamic process. In the initial frame ($t = 0$ min), the wormlike assembly of **5a** is randomly distributed. In the second frame ($t = 10$ min), below the reference point and on the lower left corner, two areas of more ordered arrangement are formed. Thirty minutes later, ordered assembling structures of **5a** begin to appear on the whole image in Figure 4c. The small domains marked as A, B, C, D, and E extend to form

larger areas (Figure 4c–f). The molecules in the area circled in Figure 4d–f reorient with respect to the adjacent domains. At domain boundaries, molecules are often not ideally close-packed, and the free volume within these areas is significantly increased compared with that in the ordered domains.[25] This can be deduced from the fact that, in STM images, domain boundaries indicated by the red arrows in the images assume fuzzy appearances. The molecular motion in the adlayer is the

main reason for these blurry images. On the basis of the theory of Ostwald ripening,[26] the thermodynamic driving force is the reduction of the circumference-to-area ratio and thereby the lowering of the interfacial or line energy. Due to the relatively large free volume, individual molecules or lamella fragments at the domain boundary can change their orientations with respect to the underlying substrate to obtain a commensuration with the lattice of graphite, and this will lead to a minimization of the free energy of the whole system.

Owing to its important influence on material properties, the epitaxial alignment of molecules in van der Waals epitaxy on a variety of surfaces has been studied.[27,28] On the basis of analyses of numerous reported epitaxial molecular films, coincidence is quite common, even though it is not as energetically favorable as commensurism based on overlayer−substrate interface energies alone. In the current system of **5a**, the 60/120° orientation of the domains (Figure 4f) clearly indicates a commensurate adsorption of the alkyl chain with the graphite lattice. At the same time, the emergence of the 90° orientation of domains is amusive. From the high-resolution STM image, it is obvious that the 90° orientation is caused by enantiomeric packing of **5a**. Many studies have shown that a substrate surface can be used as a symmetry-breaking agent to induce enantiomorphic ordering in assemblies produced even by depositing achiral molecules.[29−31] When **5a** adsorbs onto a graphite surface, rotation of the C−C bond connecting the alkyl "tail" to the isophthalic acid "head" becomes strongly hindered. This rotational barrier imparts to the molecule a new chiral center. As a result, **5a** molecules form "mirror" domains on the surface. Visualization of the underlying graphite lattice clearly illustrates that the alkyl chains in both of these domains adsorb commensurate with the graphite lattice.

5. Discussion. In the case of **5b,** it needs more time than **5a** to form ordered packing. As for **5c,** under the applied experimental conditions no long-range order has been observed. The dynamic behavior as described above can be speculated to be due to a correlated desorption and re-adsorption process of molecules, which allows the system to reach a minimum of free energy. This process can be divided into two stages. At short exposure time, the increase in coverage is very fast and can be ascribed to random physisorption of the molecules without any particular ordering. With the increasing of time, the molecules are able to reorient to obtain an ordering arrangement with a registry of alkyl chains with respect to graphite lattices.

We cannot completely rule out the influence of STM tip on the molecular motion, but it is inferred that tip−molecule interaction is not essential for the molecular motion in this system because the STM images reflecting the molecular motion were observed regardless of the operating conditions such as bias voltage, tunneling current, and scanning rates.[32,33] In addition, by a simple experimental operation, we could prove that the STM tip has little effect on the molecular motion. After the dynamic observation is completed and the ordered domains are formed, the scanning area is suddenly enlarged, for example, from 100 × 100 nm to 200 × 200 nm. If the tip effect is essential for this ordering process, we would visualize a 100 × 100 nm ordered square surrounded by disordered structures, but in fact this has not been observed in the experiment. What we discovered is a 200 × 200 nm ordered monolayer. Thus, this operation could directly prove that the tip effect is not essential for the observed dynamic process.

When molecules adsorb onto the flat solid substrate, the molecule−molecule and molecule−substrate interactions play an important role in determining the final arrangement of self-assembly. The conformation and the monolayer arrangement of these molecules are strongly affected by the intermolecular forces, which are structural driving forces in the self-assembly of monodendron molecules. The key structural elements of these three mondendrons in this study consist of carboxyl functional groups at the focal point for hydrogen bonding and alkyl tails for the stabilization of assembled structures via van der Waals interactions.[34] The only difference of these molecules is the number of peripheral alkyl chains. As for **5a** and **5b**, the aromatic cores and alkyl chains are closely packed in the assembling structure. This kind of close packing of alkyl chains and the hydrogen bonds formed among four neighboring molecules favor the stability of the assembly. In the case of **5c**, due to the increased number of alkyl substituents, the aromatic cores of neighboring molecules are separated, and hydrogen bonding between carboxyl groups of adjacent molecules is hindered, this leads to a decrease in the stability of the assembly. On the other hand, to obtain a close packing of alkyl chains, several C−C bonds on the alkyl chains will endure bond torsion, especially in the case of **5c**; the steric hindrance caused by bond torsion is extremely large. This also leads to the lack of long-range order in the assembly of **5c**.

Conclusion

The well-organized 2D monolayer structures of three alkylated 5-(benzyloxy)-isophthalic acid derivatives were studied by STM. The arrangements of the molecules with one and two alkyl substitutents are different, with alkyl chains interdigitating and packing tail (alkyl chain)-to-tail, respectively. The molecule−molecule and molecule−substrate interactions both play important roles in determining the final arrangement of self-assembly. As for the three-chain derivative, no ordered arrangement in a large area was observed, due to the steric hindrance caused by bond torsion with the increase of the alkyl chains. Take **5a** for example; we

(25) Stabel, A.; Heinz, R.; DeSchryver, F. C.; Rabe, J. P. *J. Phys. Chem.* **1995**, *99*, 505.

(26) De Feyter, S.; Gesquière, A.; Abdel-Mottaleb, M. M.; Grim, P. C. M.; DeSchryver F. C. *Acc. Chem. Res.* **2000**, *33*, 525.

(27) Hooks, D. E.; Fritz, T.; Ward, M. D. *Adv. Mater.* **2001**, *13*, 227.

(28) Lei, S. B.; Yin, S. X.; Wang, C.; Wan, L. J.; Bai, C. L. *Chem. Mater.* **2002**, *14*, 2837.

(29) Weckesser, J.; Vita, A. D.; Barth, J. V.; Cai, C.; Kern, K. *Phys. Rev. Lett.* **2001**, *87*, 096101.

(30) Kühnle, A.; Linderoth, T. R.; Hammer, B.; Besenbacher, F. *Nature* **2002**, *415*, 891.

(31) Barth, J. V.; Weckesser, J.; Trimarchi, G.; Vladimirova, M.; Vita, A. D.; Cai, C.; Brune, H.; Günter, P.; Kern, K. *J. Am. Chem. Soc.* **2002**, *124*, 7991.

(32) Hibino, M.; Sumi, A.; Hatta, I. *Thin Solid Films* **1996**, *281−282*, 594.

(33) Padowitz, D. F.; Sada, D. M.; Kemer, E. L.; Dougan, M. L.; Xue, W. A. *J. Phys. Chem. B* **2002**, *106*, 593.

(34) Kim, C.; Kim, K. T.; Chang, Y. *J. Am. Chem. Soc.* **2001**, *123*, 5586.

observed in real time the dynamic process of disorder−order transition in the monolayer. The result can be explained by the minimization of the free energy in the whole system. The research on self-assembled monolayers of dendrimers is of significant importance. The new discoveries and developments in chemistry, materials science, and biology involving dendrimers at surfaces and interfaces could be anticipated.

CM030289U